A Method for the Selective Reinforcement of Natural Fiber Composites Considering Manufacturing Constraints

Niklas Frank(✉), Simon Voltz, Albert Albers, and Tobias Düser

IPEK - Institute of Product Engineering at Karlsruhe Institute of Technology (KIT), Karlsruhe, Germany
niklas.frank@kit.edu

Abstract. Natural fiber composites (NFC) present a promising approach to cope with current challenges caused by the climate change, such as resource scarcity and the need to reduce carbon dioxide emissions. However, the comparatively poor mechanical properties of natural fibers require an intelligent solution to achieve sufficient component stiffness. One possible approach are hybrid NFC by combining natural fibers with carbon fiber (CF) tapes. In this work, a method for the calculation of load path-oriented CF tapes for the selective reinforcement of NFC components is proposed. Unidirectional stress states are identified and combined by means of a stress cluster algorithm. Criteria to evaluate the orientation and stress effectiveness of stress clusters are defined. Finally, selected stress clusters are approximated by the geometry of the CF tapes considering the manufacturing constraints of the dry fiber placement process. Selective reinforcements are calculated for a seat structure and compared with other reinforced seat designs. Further research to extend the proposed method is suggested.

Keywords: natural fiber composites · stress cluster · local reinforcement · manufacturing constraint

1 Introduction

In recent years, climate change has still steadily gained in importance. In particular, resource scarcity and the need to reduce carbon dioxide emissions continue to pose a difficult challenge. Although lightweight design could be a possible solution to these problems, synthetic fibers such as carbon fibers (CF) are often used, which are associated with high energy consumption and carbon dioxide emissions in the production process [7,11,18]. Here, natural fiber composites (NFC) present a promising alternative for the design of lightweight structures. Natural fibers (NF) are a renewable resource, require little energy in production and have a high weight-specific stiffness [10,16]. However, the mechanical properties of CF are superior to those of NF [17]. In addition, NF have a high moisture absorption, which leads to a reduction of mechanical properties [16]. Also, the material characteristics are subject to high scattering [1]. Because of

these drawbacks, most applications of NFC are limited to non-structural, barely loaded parts [10]. Current research is focusing on extending the scope of NFC to (semi-) structural components. In [3] the reinforcement of NFC by the tailor fiber placement (TFP) process was investigated, using NF and CF as additional reinforcement fibers. In both cases, an increase in the flexural modulus was achieved, although a higher reinforcement was observed with CF. In further research, locally reinforced NFC using unidirectional CF tapes manufactured with the dry fiber placement (DFP) process [14] will be investigated [3]. For material-appropriate recycling paths, these CF tapes need to be separated from the NFC at the end of life using an energy-intensive laser process. Hence, a design method for the calculation of only a few additional reinforcement tapes needs to be developed.

Although there are many works on the load path-oriented design of composite parts (e.g. [6,9,19–21]), only a few deal with the calculation of local reinforcements of composites. Reference [12] and [22] consider the local reinforcement of an open hole plate using TFP. The fiber paths were calculated based on the principal stress trajectories. In [5] a method for the local reinforcement in the context of tailored textiles is presented. After separating the reinforcement area from the base lamina, stress clusters are calculated using k-means clustering based on the first and second principal stress directions.

To the best of the author's knowledge, there is no work on the design of selectively reinforced, three-dimensional NFC components using CF tapes considering the DFP process. Therefore, we propose a method for the calculation of load path-oriented CF tapes for the selective reinforcement of NFC components.

2 Method

In this chapter, a detailed explanation of the proposed method is given. The method is based on the anisotropy criterion described in [8] to identify unidirectional stress states. Then, areas with these specific stress states are combined by means of a stress cluster algorithm, which is applied on maximum principal stress directions. Therefore, the method consists of several consecutive steps as shown in Fig. 1. These steps can be collectively described as a preprocessing step (model building, calculation of anisotropy criteria and surface preparation), followed by a stress cluster step and finally a postprocessing step (cluster evaluation and approximation of tape geometry). The rest of this section is structured according to these steps, each of which is discussed in detail.

2.1 FE Model

For a better understanding and visualization of the following steps of the method, a seat structure with a simple load case as depicted in Fig. 2 is defined. A finite element model is created considering the plane symmetry of the loaded structure. For the NFC, a quasi-isotropic lay-up is assumed. Since the global deformation behavior is of interest, the NFC is simplified and modeled as an isotropic, homogeneous material. Furthermore, for some surfaces no reinforcement is desired,

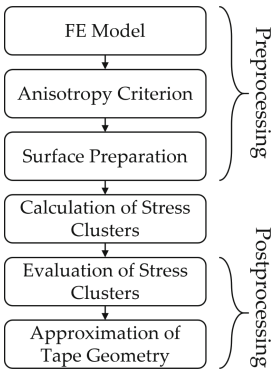

Fig. 1. Flowchart of the proposed method

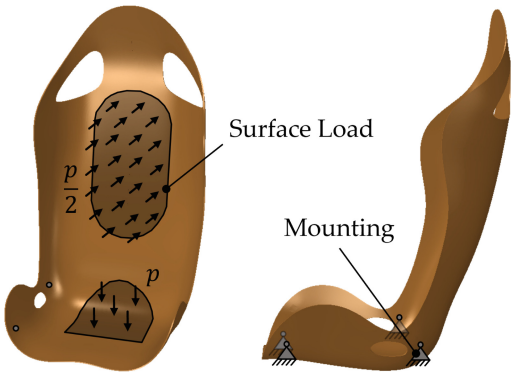

Fig. 2. Load case of the seat structure

e.g. on thin edges or because of aesthetic reasons. These surfaces can be deselected and are not considered in the next steps of the proposed method. A constraint for the seat structure is that reinforcement tapes may only be placed on the back.

2.2 Anisotropy Criterion

The proposed method is based on the anisotropy criterion developed in [8]. For this criterion, an anisotropy value K is defined, measuring the stress state in each element based on the principal stresses $\boldsymbol{\sigma}_{\mathrm{I}}$, $\boldsymbol{\sigma}_{\mathrm{II}}$ and $\boldsymbol{\sigma}_{\mathrm{III}}$

$$\mathrm{K} = \left(\frac{\max(|\boldsymbol{\sigma}_I|, |\boldsymbol{\sigma}_{II}|, |\boldsymbol{\sigma}_{III}|)}{|\boldsymbol{\sigma}_I| + |\boldsymbol{\sigma}_{II}| + |\boldsymbol{\sigma}_{III}|} - \frac{1}{3} \right) \frac{3}{2} \in [0; 1]. \tag{1}$$

A value close to $K = 1$ represents an unidirectional stress state, whereas a value close to $K = 0$ represents a strongly non-unidirectional stress state, i.g. all principal stresses are almost equal ($\boldsymbol{\sigma}_{\mathrm{I}} \approx \boldsymbol{\sigma}_{\mathrm{II}} \approx \boldsymbol{\sigma}_{\mathrm{III}}$). The distribution of the anisotropy values for the seat structure is shown in Fig. 3.

2.3 Surface Preparation

The anisotropy values are used to identify elements with a near-unidirectional stress state. In order to combine these in a subsequent cluster step, the surface of the structure is first divided into several contiguous surfaces with similar normal vectors. The reason for this is the previously mentioned separation of the CF tapes from the NFC using a laser process, which requires a constant focal length over the entire tape length. To make this possible, the reinforcement tapes must be placed on approximately flat surfaces. This also simplifies the subsequent clustering process. However, this implies that tapes cannot be placed on curvatures and therefore longer tapes may be suppressed.

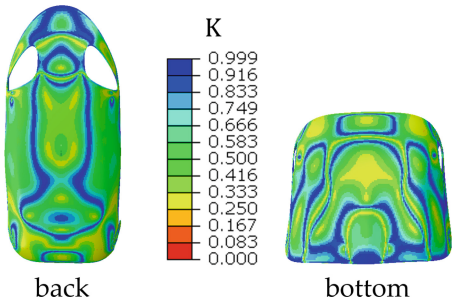

Fig. 3. Distribution of anisotropy values for the loaded seat structure

To identify contiguous, approximately flat surfaces a cluster algorithm is used. For this, the normal vector of each surface element is calculated and normalized. These vectors describe points on the surface of a unit sphere (see Fig. 4) and are used as input for the cluster algorithm. As the number of clusters is unknown, the mean shift algorithm implemented in the *scikit-learn* library [15] is chosen. The mean shift algorithm depends on only one variable, the bandwidth α. In the present case, α can be interpreted as an angular deviation in radians. Since similar normal vectors can be located at different positions (see Fig. 4), identified clusters must then be partially separated using neighborhood relations of the surface elements. In Fig. 5a the identified surfaces with similar normal vectors are shown for a bandwidth of $\alpha = 15°$.

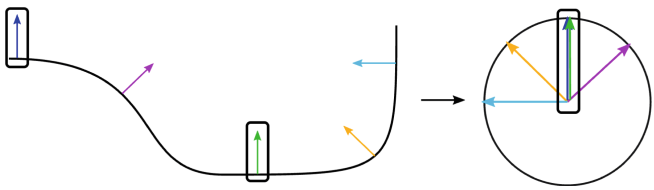

Fig. 4. Normal vectors are used to describe points on the surface of a unit sphere. For simplicity, the respective 2D case is visualized here, i.e. vectors describing points on a unit circle

Each identified surface is then filtered using the calculated anisotropy values, i.e. elements with an anisotropy value less than a minimum value ($K < K_{\min}$) are not considered further. The filtering of the subdivided surfaces for a minimum anisotropy value of $K_{\min} = 0.5$ and $K_{\min} = 0.7$ is shown in Fig. 5. The choice of $K_{\min}$ is very important, as all surface elements remaining after filtering are used as input for the subsequent stress clustering. If the minimum value is too large, small and narrow stress clusters tend to occur, while smaller minimum values result in greater deviations from the unidirectional stress state.

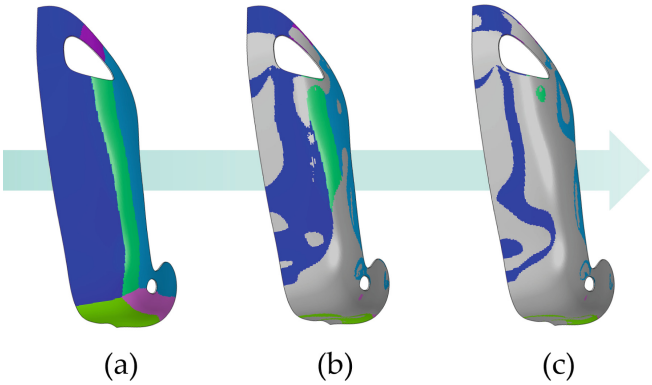

Fig. 5. Results of clustering surfaces with similar normal vectors and subsequent filtering with $K_{\min}$. Each color represents a cluster. **a** Clustered surfaces with similar normal vectors **b** Filtered surfaces with $K_{\min} = 0.5$. **c** Filtered surfaces with $K_{\min} = 0.7$

2.4 Calculation of Stress Clusters

In the next step, principal stress clusters are calculated for each of the filtered surface elements. By normalizing the maximum principal stress vectors, these can again be seen as points on the surface of a unit sphere. Therefore, the same clustering procedure as described in Sect. 2.3 can be employed. Afterwards, the stress clusters are separated according to their geometric position using neighborhood relations (see Fig. 6). Finally, the reinforcement direction of the UD tape $\boldsymbol{v}_{\mathrm{c}}$ is calculated for each cluster by averaging the principal stress vectors $\boldsymbol{v}_{\mathrm{e}}$ of the corresponding elements. In Fig. 7 the identified stress clusters are shown for a bandwidth of $\alpha = 30°$.

2.5 Evaluation of Stress Clusters

The result of the stress cluster analysis is a large number of clustered surface elements that have an unidirectional stress state in approximately the same direction. Since only a few effective clusters should be used, suitable evaluation criteria are required. For this purpose, clusters with a small area ($A < A_{\min}$) are initially sorted out, as tape reinforcement can already be ruled out for these in advance. In addition, numerical inaccuracies result in many small clusters that only contain a few elements (1–10) and are consequently also sorted out in this way. Further, two evaluation criteria are defined: orientation and stress effectiveness.

The orientation effectiveness $E_\theta \in [0.086; 1]$ evaluates the deviation of the principal stress vector of the respective elements in a cluster from the averaged cluster reinforcement vector. The deviation θ is calculated as an average over N elements within a cluster

$$\theta = \frac{\sum_{\mathrm{e}=1}^{N} \cos^{-1}\left(\frac{\vec{v}_{\mathrm{e}} \cdot \vec{v}_{\mathrm{c}}}{|\vec{v}_{\mathrm{e}}||\vec{v}_{\mathrm{c}}|}\right)}{N}. \tag{2}$$

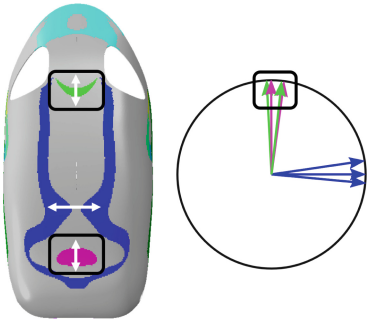

Fig. 6. Visualization of the clustering process of principal stress vectors. Each color represents an identified cluster of similar maximum principal stress vectors. White arrows represent the averaged principal stress vector within a cluster

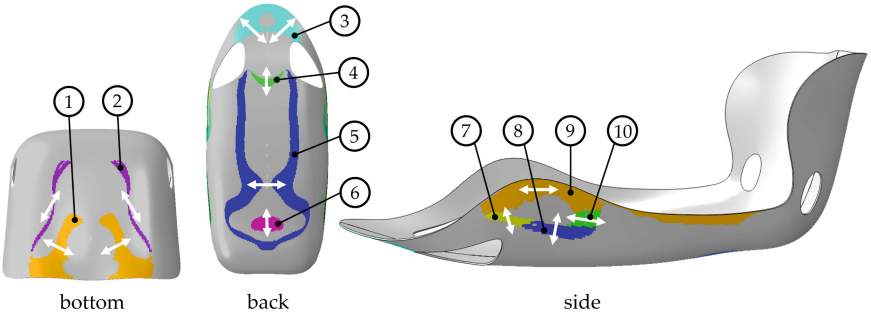

Fig. 7. Result of stress clustering. Each color represents an identified cluster of similar maximum principal stress vectors. White arrows represent the averaged principal stress vector within a cluster

Using this average deviation angle, E_θ is calculated using the stiffness loss shown in [13] due to the deviation of the fiber orientation from the load direction (see Fig. 8).

The stress effectiveness $E_\sigma \in [0;1]$ evaluates the possible stiffness gain based on the principal stress magnitude. This is necessary because a cluster may have a perfectly unidirectional stress state, but at the same time may be located in an area with low stress magnitudes and therefore not represent any added value. The stress effectiveness is calculated relative to all M clusters. The averaged maximum principal stress $\boldsymbol{\sigma}_{\mathrm{I_c}}$ is calculated for each cluster and set in relation to the cluster with the largest occurring averaged maximum principal stress, i.e. there is always a cluster with $E_\sigma = 1$

$$\boldsymbol{\sigma}_{\mathrm{I_c}} = \frac{\sum_{\mathrm{e}=1}^{N} \boldsymbol{\sigma}_{\mathrm{I_e}}}{N}, \tag{3}$$

$$E_\sigma = \frac{\boldsymbol{\sigma}_{\mathrm{I_c}}}{\max(\boldsymbol{\sigma}_{\mathrm{I_c}} : \mathrm{c} = 1, ..., M)}. \tag{4}$$

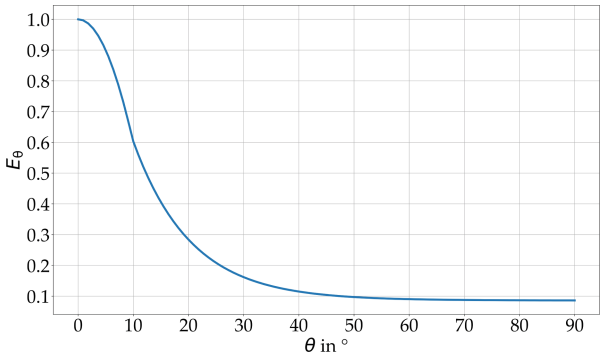

Fig. 8. Stiffness reduction due to the deviation of the fiber orientation from the load direction according to [13]

In Table 1 the calculated effectiveness values for the resulting stress clusters (Fig. 7) are shown. These values can be used to support the product developer in the design process of the reinforcement or to automatically select only a few efficient clusters. Based on the efficiency values calculated for the seat structure and assigning a stronger weight for E_σ, stress clusters 2,5,6 and 9 could be chosen for the reinforcement.

Table 1. Calculated effectiveness values for the stress clusters in Fig. 7

Cluster number	1	2	3	4	5	6	7	8	9	10
E_θ	0.59	0.61	0.62	0.97	0.34	0.97	0.42	0.67	0.68	0.79
E_σ	0.45	0.74	0.51	0.42	0.69	1.00	0.33	0.41	0.98	0.49

2.6 Approximation of Tape Geometry

Other than the evaluation of the stress clusters with the criteria mentioned before, the manufacturing constraints regarding the DFP process need to be considered as well. Firstly, fiber tapes are placed with a constant width b and a minimum length $l_{\min}$. Secondly, the required two-dimensional placement path for each tape must be calculated.

Since the reinforcement areas are present in complex shapes after clustering, they must be approximated by the geometry of the reinforcement tapes, i.e. rectangles. This approximation problem can be greatly simplified, as described in the following. First, the outline of a cluster, which can be described by a sequence of points, is projected onto a plane. This is admissible because the clusters are calculated on the surfaces subdivided in advance, which have a similar normal vector. In this plane, the outline of a cluster is described by a polygon using a two-dimensional coordinate system. The polygon is then rotated so that the

averaged cluster reinforcement direction coincides with one of the two axes of the coordinate system in the plane. Starting from the center axis of the bounding box of the polygon, several slices are created within the box, using the specified width of a reinforcement tape (see Fig. 9).

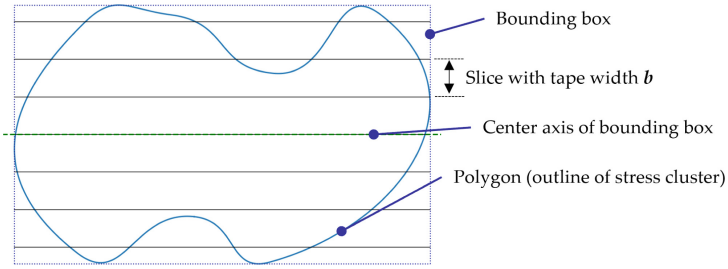

Fig. 9. Starting from the center axis of the bounding box of a polygon, several slices with the specified tape width b are created.

After this simplification, the approximation of the tape geometry can be seen as an optimization problem with an objective function for each slice

$$A_{\text{covered},i}(x_i, l_i) = A_{\text{poly}} \cap A_{\text{rect},i}, \tag{5}$$

$$A_{\text{overlap},i}(x_i, l_i) = A_{\text{rect},i} - A_{\text{covered},i}(x_i, l_i), \tag{6}$$

$$f = \sum_{i=1}^{n_{\text{rect}}} (A_{\text{covered},i}(x_i, l_i) - A_{\text{overlap},i}(x_i, l_i)). \tag{7}$$

For each slice, the horizontal position x_i and length l_i of an unknown number of rectangles n_{rect} is searched, such that the covered polygon area is maximized while minimizing the area of rectangles not covering any polygon area.

To solve this optimization problem a heuristic approach is used. Each slice is divided into two equal rectangles in an iterative manner, i.e. created rectangles are divided as well, an so on. To improve the performance of this approach, for each slice a binary tree is created. Each node represents a rectangle that can be divided into two other nodes (rectangles). If a rectangle fulfills either $g = 0$ or $g = 1$, the corresponding node no longer has to be considered

$$g = \frac{A_{\text{covered}}}{A_{\text{rect}}}. \tag{8}$$

Furthermore, each binary tree can be seen as an independent optimization problem, thus allowing parallelization. A stop criterion for the subdivision process is defined for each branch by means of a maximum tree depth. Finally, for each slice tapes can be recovered by traversing the leaves and combining the corresponding rectangles (see Fig. 10).

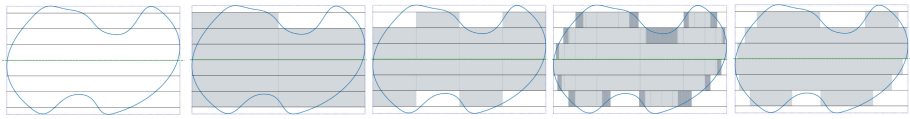

Fig. 10. Visualization of the subdivision process. Each rectangle is subdivided until either $g = 0$, $g = 1$ or maximum tree depth is reached. Afterwards all rectangles are connected to tapes by traversing the leaves

In Fig. 11 and Fig. 12 the approximated tape geometries for some stress clusters of the seat structure can be seen. Tapes with a length less than a specified minimum ($l < l_{\min}$) are deleted. The required two-dimensional placement path for each tape can be obtained with the center lines of the respective rectangles. It can be seen that by using this heuristic approach, complex polygon shapes can be approximated in an acceptable manner. Also, for very narrow clusters, DFP does not present a suitable manufacturing process (see Fig. 12).

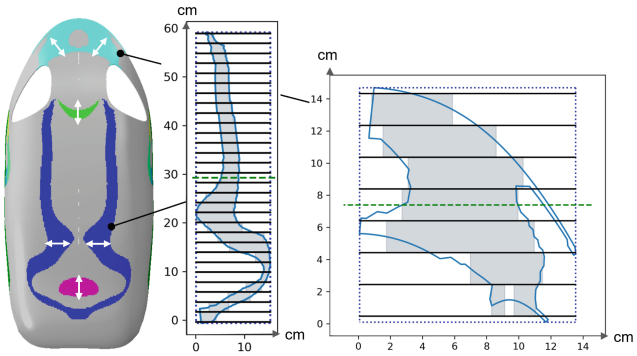

Fig. 11. Approximation of tapes geometries for stress cluster at the back of the seat structure

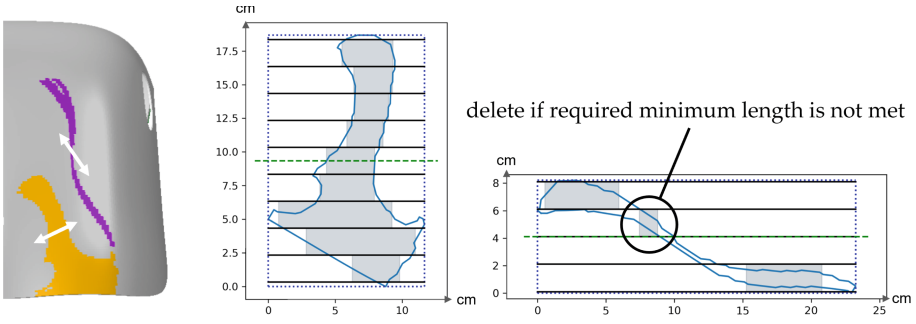

Fig. 12. Approximation of tapes geometries for stress clusters at the bottom of the seat structure

3 Results and Comparison of Reinforcement Designs

In this work a method was presented for the design of selective reinforcements of three-dimensional NFC components using CF tapes. A comparison to other standard reinforcement designs is given in Fig. 13. Here, Fig. 13b shows the result of a conventional design process based on experience. Another approach to reinforce NFC is shown in Fig. 13c. The grid-like reinforcement is known as powerRibs^{TM} [4] and is manufactured by Bcomp®. In this case, NF are used for the additional reinforcement. There are clear differences between all reinforcement variants. In particular, in comparison to the conventional approach, the proposed method calculates additional reinforcement areas on the side and bottom of the seat structure. It can also be observed that the proposed method generates rather short tape lengths, whereas the other designs favor a continuous fiber reinforcement. It is important to note that a simple load case was chosen for the seat structure and the calculated stress clusters will likely change if the load case is modeled differently.

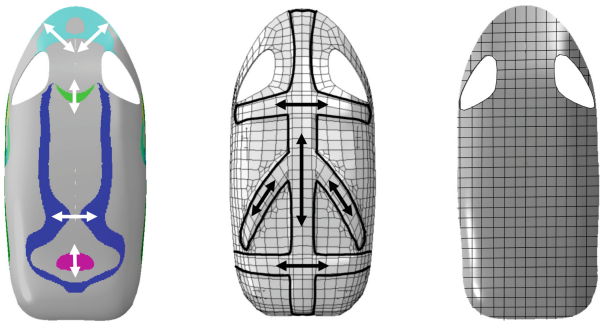

Fig. 13. Comparison of reinforcement designs. **a** Reinforcement of proposed method. **b** Reinforcement of conventional design process [2]. **c** Reinforcement with powerRibs^{TM} [4]

4 Conclusion and Outlook

In a next step, detailed FE models of the different reinforcement design variants shown in Fig. 13 will be created to compare the respective weight-specific stiffness. For now, the method creates a basis for further optimization of selective reinforced NFC. A few drawbacks can already be identified and will be addressed in further studies. Using topology optimization to identify load paths as a preliminary step of this method might result in longer reinforcement tapes. Because of the weak mechanical properties of the NFC, a reinforcement approach to additionally consider failure criteria of the NFC will be investigated. As seen in the

tape approximation step, some clusters have a narrow outline and consequently are not suitable for tape reinforcement. Hence, the proposed method will be extended to additionally consider the TFP process.

Acknowledgment. We would like to thank the Ministry of Science, Research and Arts Baden-Württemberg and the InnovationCampus Future Mobility (ICM) for funding the research. The results presented were produced as part of the ICM project EM7 - DefoRe (Design for Recycling). Our cooperation with the Institute of Aircraft Design (IFB) and the Institut für Strahlwerkzeuge (IFSW) of the University of Stuttgart is particularly noteworthy.

References

1. Akampumuza, O., Wambua, P.M., Ahmed, A., Li, W., Qin, X.: Review of the applications of biocomposites in the automotive industry. Polym. Compos. **38**(11), 2553–2569 (2016). https://doi.org/10.1002/pc.23847
2. Baur, J.: Conventional design of a reinforced seat structure (2022)
3. Baur, J., Helber, F., Middendorf, P., Strohl, C., Graf, T.: Untersuchungen zu Herstellung, Einsatz und Recycling von nachhaltigen FVK. 28. Stuttgarter Kunststoffkolloquium (2023)
4. Bcomp: powerRibs™ natural fibre reinforcement for high performance (2024). https://www.bcomp.ch/products/powerribs/
5. Berges, J.M., Jacobs, G., Stein, S., Sprehe, J.: Methodology for the concept design of locally reinforced composites. Appl. Sci. **11**(16), 7246 (2021). https://doi.org/10.3390/app11167246
6. Bittrich, L., Spickenheuer, A., Almeida, J.H.S., Müller, S., Kroll, L., Heinrich, G.: Optimizing variable-axial fiber-reinforced composite laminates: the direct fiber path optimization concept. Math. Probl. Eng. **2019**, 1–11 (2019). https://doi.org/10.1155/2019/8260563
7. Das, S.: Life cycle assessment of carbon fiber-reinforced polymer composites. Int. J. Life Cycle Assess. **16**(3), 268–282 (2011). https://doi.org/10.1007/s11367-011-0264-z
8. Durst, K.G.: Beitrag zur systematischen Bewertung der Eignung anisotroper Faserverbundwerkstoffe im Fahrzeugbau. Dissertation, Universität Stuttgart, Stuttgart (2008)
9. Eckrich, M., Arrabiyeh, P.A., Dlugaj, A.M., May, D.: Structural topology optimization and path planning for composites manufactured by fiber placement technologies. Compos. Struct. **289**, 115488 (2022). https://doi.org/10.1016/j.compstruct.2022.115488
10. Elseify, L.A., Midani, M., El-Badawy, A., Jawaid, M.: Manufacturing Automotive Components from Sustainable Natural Fiber Composites. Springer, Cham (2021). https://doi.org/10.1007/978-3-030-83025-0
11. Ghosh, T., Kim, H.C., de Kleine, R., Wallington, T.J., Bakshi, B.R.: Life cycle energy and greenhouse gas emissions implications of using carbon fiber reinforced polymers in automotive components: front subframe case study. Sustain. Mater. Technol. **28**, e00263 (2021). https://doi.org/10.1016/j.susmat.2021.e00263
12. Gliesche, K., Hübner, T., Orawetz, H.: Application of the tailored fibre placement (TFP) process for a local reinforcement on an "open-hole" tension plate from carbon/epoxy laminates. Compos. Sci. Technol. **63**, 81–88 (2003). https://doi.org/10.1016/S0266-3538(02)00178-1

13. Klein, D., Caballero, S., Wartzack, S.: Berechnung beanspruchungsgerechter Faserorientierungen in CFK-Strukturen. In: ANSYS Conference & 31. CADFEM Users Meeting (2013)
14. Kühn, F., Rehra, J., May, D., Schmeer, S., Mitschang, P.: Dry fiber placement of carbon/steel fiber hybrid preforms for multifunctional composites. Adv. Manuf. Polym. Compos. Sci. **5**(1), 37–49 (2019). https://doi.org/10.1080/20550340.2019.1585027
15. Pedregosa, F., et al.: Scikit-learn: machine learning in Python. J. Mach. Learn. Res. **12**, 2825–2830 (2011)
16. Pickering, K.L., Efendy, E.M., Le, T.M.: A review of recent developments in natural fibre composites and their mechanical performance. Compos. Part A Appl. Sci. Manuf. **83**, 98–112 (2016). https://doi.org/10.1016/j.compositesa.2015.08.038
17. Shamsuyeva, M., Hansen, O., Endres, H.J.: Review on hybrid carbon/flax composites and their properties. Int. J. Polym. Sci. **2019**, 1–17 (2019). https://doi.org/10.1155/2019/9624670
18. Suzuki, T., Takahashi, J.: Prediction of energy intensity of carbon fiber reinforced plastics for mass-produced passenger cars. In: Japan International SAMPE Symposium, vol. 9, pp. 14–19 (2005)
19. Tanaka, H., Mori, Y., Kumekawa, N., Matsuzaki, R.: Multi-objective optimization of weight and strength of laminated composites using gap-less and overlap-less variable thickness fiber placement. Compos. Struct. **276**, 114562 (2021). https://doi.org/10.1016/j.compstruct.2021.114562
20. Tanaka, H., Mori, Y., Kumekawa, N., Matsuzaki, R.: Optimization of fiber orientation and layer thickness in thin carbon fiber-reinforced plastic curved structures. Compos. Part C Open Access **12**, 100381 (2023). https://doi.org/10.1016/j.jcomc.2023.100381
21. Zhao, S., Wu, N., Wang, Q.: Load path-guided fiber trajectory in composite panels: a comparative study and a novel combined method. Compos. Struct. **263**, 113689 (2021). https://doi.org/10.1016/j.compstruct.2021.113689
22. Zhu, Y., Qin, Y., Qi, S., Xu, H., Liu, D., Yan, C.: Variable angle tow reinforcement design for locally reinforcing an open-hole composite plate. Compos. Struct. **202**, 162–169 (2018). https://doi.org/10.1016/j.compstruct.2018.01.021